Eur. Phys. J. A **17**, 145–152 (2003)
DOI 10.1140/epja/i2001-10272-2

THE EUROPEAN PHYSICAL JOURNAL A

Subthreshold K^--meson production in proton-nucleus reactions revisited

E.Ya. Paryev[a]

Institute for Nuclear Research, Russian Academy of Sciences, Moscow 117312, Russia

Received: 26 July 2001 / Revised version: 23 December 2002 /
Published online: 8 April 2003 –
Communicated by V. Vento

Abstract. We study the inclusive K^--meson production in proton-nucleus collisions in the subthreshold energy regime in the framework of a spectral function approach for incoherent primary proton-nucleon and secondary pion-nucleon production processes. Our approach takes properly into account the effect of the nuclear mean-field potentials on these processes, as well as the final-state interaction (FSI) among the outgoing nucleons participating in the one-step antikaon creation process. A detailed comparison of the model calculations of the K^- differential cross-sections for the reactions $p+{}^{9}$Be, $p+{}^{63}$Cu, and $p+{}^{197}$Au at subthreshold energies with the currently available experimental data obtained recently at the ITEP proton synchrotron and at SIS/GSI is given. We find that our calculation, which includes both the nuclear density-dependent mean-field potentials and the elementary NN-FSI effects on the K^- production from the direct mechanism, is able to reproduce the energy dependences of the invariant differential cross-sections for the "hard" antikaon creation in p-^{9}Be and p-^{63}Cu collisions. This result contradicts previous estimates which used only density-dependent mean fields in calculating the K^- yield from this mechanism. We further show that the NN-FSI effects play a minor role in describing the data on the spectrum of the relatively soft K^--mesons from p-^{197}Au interactions at incident energy of 2.5 GeV. We find that the relative strength of the proton- and pion-induced reaction channels in the subthreshold energy regime is governed by the kinematics of the experiment under consideration. We also explore the influence of the antikaon mean-field potential on the K^- yield at low antikaon momenta.

PACS. 25.40.-h Nucleon-induced reactions

1 Introduction

In a recent publication [1] the possibility to describe the first experimental data [2] on subthreshold antikaon production in p-^{9}Be and p-^{63}Cu collisions within the spectral function approach has been investigated. This description is based both on the direct mechanism of the K^- production and on the two-step mechanism associated with the creation of antikaons by intermediate pions. Within such an approach the measured yields of rather "hard" K^--mesons with a momentum of 1.28 GeV/c at a laboratory angle of 10.5° from $p+{}^{9}$Be and $p+{}^{63}$Cu reactions are reproduced quite well at beam energies $\epsilon_0 > 2.4$ GeV by calculations which, for the primary production process $pN \to NNKK^-$ (the dominant one), use attractive nucleon and antikaon density-dependent effective potentials. At lower bombarding energies the experimental results are underestimated by these calculations. The use of the corresponding density-independent fields with depths taken at nuclear saturation density ρ_0, significantly improves the agreement of calculations with the data in the far subthreshold energy region (at energies $\epsilon_0 \leq 2.4$ GeV), but overestimates the data by a factor of 2 at higher incident energies. Evidently, the use of the density-independent mean-field potentials in the calculations of ref. [1] for the one-step reaction channel $pN \to NNKK^-$ allows one to get an upper estimate of the respective cross-sections. In this case the enhancement of the K^- production via the above channel is maximal since the (density-independent) shift of the elementary production threshold to lower energy is the largest, and the available phase space, of the unobserved NNK system (which determines the K^- differential cross-section in pN collisions), becomes maximal for the smallest density-independent masses of the final nucleons. In fact a certain averaging of the antikaon production over all densities $\rho_N \leq \rho_0$ takes place. Therefore, the existing disagreement between the calculations of ref. [1] with the nuclear density-dependent potentials and the data of ref. [2] at energies far below the free K^- production threshold indicates that higher-order processes might play an important role. Taking into consideration that in

[a] e-mail: Paryev@a120.INR.Troitsk.ru

the far subthreshold energy region the relative momenta of the outgoing particles (two nucleons and kaon) participating in the primary proton-induced reaction channel $pN \to NNKK^-$ are small, the latter discrepancy might be entirely due to a final-state interaction (FSI) effect between them (mainly among the final nucleons, since the KN interaction is known to be rather weak in comparison with the strong NN interaction). Such a FSI effect may greatly modify the angular-momentum distribution of antikaons produced in this channel. This effect was neglected in ref. [1] in the calculation of the "in-medium" differential cross-section for the K^- production in pN collisions for the kinematics of the experiment in ref. [2]. It is the purpose of the present study to address these issues by computing this cross-section using the Watson-Migdal FSI theory [3–5], as well as, by reanalyzing the data in ref. [2] employing the new cross-section in the calculations for the direct antikaon production mechanism. Furthermore, new experimental data on the subthreshold K^- production in p-^{197}Au interactions have been obtained recently by the KaoS Collaboration at SIS/GSI [6]. Namely, the double differential cross-section for the K^- production at a lab angle of 40° in $p + {}^{197}$Au collisions at 2.5 GeV beam energy has been measured in ref. [6]. The aim of this paper is also to present an analysis of these data using the spectral function approach in ref. [1] that has been modified, in line with the above-mentioned arguments to account for the NN-FSI effects in the primary creation process. It is clear that such an analysis will permit to improve our understanding of the phenomenon of the subthreshold antikaon production in composite hadronic systems. In this paper we also present our predictions for the differential cross-section for the K^- production using ^{9}Be as target nucleus at 2.25 GeV incident energy, which might be measured, for example, at the ITEP proton synchrotron or at the Cooler Synchrotron COSY-Jülich. The spectral function approach is explained in detail in ref. [1], we briefly recall the main assumptions here and describe the respective modifications.

2 The model

Apart from participating in the elastic scattering an incident proton can produce a K^- directly in the first inelastic pN collision due to nucleon's Fermi motion. Since we are interested in the few-GeV region (up to 3 GeV), we have taken into account the following elementary process which requires the least amount of energy and, hence, has the lowest free production threshold:

$$p + N \to N + N + K + K^- \,, \tag{1}$$

where $\{NNK\}$ stands for $\{ppK^+\}$, $\{ppK^0\}$, or $\{pnK^+\}$ for the specific isospin channel. As in ref. [1], in the following calculations we will include the medium modification of the final hadrons (nucleons, kaon, and antikaon) participating in the production process (1) by using their in-medium masses m_h^*

$$m_h^*(\rho_N) = m_h + U_h(\rho_N), \tag{2}$$

which include the effective scalar density-dependent potentials $U_h(\rho_N)$ determined in [1] (formulas (4)-(9)). We also take into account in the calculation of the K^- production cross-section from the one-step process (1) the influence of the nuclear optical potential $V_0 \approx 40$ MeV on the incoming (with kinetic energy ϵ_0) proton [1]. In our method, the K^- production cross-section for pA collisions from the primary reaction channel (1) can be expressed as the corresponding density-averaged integral of the product of the in-medium inclusive elementary antikaon production cross-section (which was assumed to be the same for pp and pn interactions) and nucleon spectral function $P(\mathbf{p}_t, E)$ over the struck target nucleon momentum $\mathbf{p}_t$ and removal energy E [1] (Eqs. (21)-(23) from this reference). The in-medium invariant inclusive cross-section for the K^- production in the elementary process (1) has been described previously [1] by the four-body phase-space calculations not including any FSI effects between the reaction products. In the far subthreshold energy region of interest the relative momenta of the outgoing particles (two nucleons and kaon) are small. Therefore, such a FSI among them (mainly between the final nucleons, since the KN interaction is rather weak compared to the strong NN interaction) may influence strongly the energy dependence of the antikaon production cross-section measured in ref. [2]. Following the Watson-Migdal theory of FSI [3–5] for two-body processes, we assume that the total reaction amplitude $M_{pN\to NNKK^-}$ for the production process (1) factorizes approximately as [1]

$$M_{pN\to NNKK^-} = M^{(0)}_{pN\to NNKK^-} \cdot M_{\rm FSI} \,, \tag{3}$$

where $M^{(0)}_{pN\to NNKK^-}$ represents the short-ranged production amplitude which is a smooth and slowly varying function of the invariant energy $\sqrt{s}$ at beam energies of interest, while $M_{\rm FSI}$ describes the on-mass-shell elastic scattering among protons in the exit channel in line with the assumption in ref. [1] of disregarding any difference between the K^--meson production cross-sections in pp and pn interactions. Among the different ways [3–5,7–35] to account for the FSI between two particles at low relative energies we employ here the Jost approximation [4,27–35] and express $M_{\rm FSI}$ as an inverse S-wave Jost function:

$$M_{\rm FSI}(q) = \frac{1}{J_0(q)} = \frac{q + i\alpha}{q - i\beta} \,, \tag{4}$$

where q is the relative momentum of the final protons, while the parameters α and β in the absence of Coulomb force [2] are related to the S-wave pp scattering length a_0

[1] It should be pointed out that the validity of such a procedure in the meson production processes close to the threshold is a matter of current debate [7–10].

[2] Our calculations showed that the use of the Coulomb-corrected [31] effective range approximation parameters a_0^c, r_0^c in eq. (5) instead of those a_0, r_0 reduces the "low"-energy ($\epsilon_0 \le 2.5$ GeV) and "high"-energy ($\epsilon_0 > 2.5$ GeV) parts of the antikaon excitation function analyzed below only by about 13% and 7%, respectively.

and effective range r_0 as follows [4,18,28,33]:

$$\alpha = (1/r_0)[1 + (1 - 2r_0/a_0)^{1/2}],$$
$$\beta = (1/r_0)[1 - (1 - 2r_0/a_0)^{1/2}]. \quad (5)$$

Using the standard values for $a_0 = -7.81$ fm and $r_0 = 2.77$ fm [36], we get

$$\alpha = 164.35 \text{ MeV}/c,$$
$$\beta = -21.90 \text{ MeV}/c. \quad (6)$$

This parameter set will be used in our subsequent calculations. It may be noted that for large q, the amplitude $M_{\rm FSI}$ goes to unity, *i.e.*, for high relative energies the FSI is of little importance [3–5]. Finally, using eqs. (3), (4), we can write expressions (25)-(28) from ref. [1], which describe the in-medium invariant inclusive cross-section for K^- production in the elementary process (1), in the following FSI-modified form:

$$E'_{K^-}\frac{{\rm d}\sigma_{pN\to NNKK^-}[\sqrt{s},\mathbf{p}'_{K^-},\rho(\mathbf{r})]}{{\rm d}\mathbf{p}'_{K^-}} = \sigma_{pN\to NNKK^-}(\sqrt{s},\sqrt{s^*_{\rm th}})f_4^{\rm FSI}(s,\mathbf{p}'_{K^-}), \quad (7)$$

$$f_4^{\rm FSI}(s,\mathbf{p}'_{K^-}) = I_3(s_{NNK},m^*_{K^+},m^*_N,m^*_N,F_{\rm FSI})\Big/ [2I_4(s,m^*_{K^+},m^*_{K^-},m^*_N,m^*_N,F_{\rm FSI})], \quad (8)$$

$$I_3(s,m^*_{K^+},m^*_N,m^*_N,F_{\rm FSI}) = (\frac{\pi}{2})^2\int\limits_{4m^{*2}_N}^{(\sqrt{s}-m^*_{K^+})^2}\frac{\lambda(s_{NN},m^{*2}_N,m^{*2}_N)}{s_{NN}}\frac{\lambda(s,s_{NN},m^{*2}_{K^+})}{s} \times F_{\rm FSI}(s_{NN}){\rm d}s_{NN}, \quad (9)$$

$$I_4(s,m^*_{K^+},m^*_{K^-},m^*_N,m^*_N,F_{\rm FSI}) = \frac{\pi}{2}\int\limits_{4m^{*2}_N}^{(\sqrt{s}-m^*_{K^+}-m^*_{K^-})^2}\frac{\lambda(s_{NN},m^{*2}_N,m^{*2}_N)}{s_{NN}}F_{\rm FSI}(s_{NN}) \times I_3(s,m^*_{K^-},\sqrt{s_{NN}},m^*_{K^+},F_{\rm FSI}=1){\rm d}s_{NN}. \quad (10)$$

The so-called FSI enhancement factor $F_{\rm FSI}$ is given by

$$F_{\rm FSI}(s_{NN}) = \Big|M_{\rm FSI}(q)\Big|^2 = \frac{q^2+\alpha^2}{q^2+\beta^2} \quad (11)$$

and

$$q = \frac{1}{2\sqrt{s_{NN}}}\lambda(s_{NN},m^{*2}_N,m^{*2}_N). \quad (12)$$

Using (6), one may easily obtain that the enhancement factor $F_{\rm FSI}$ is equal to 46.8, 3.6, and 1.7 at relative momenta of 10, 100, and 200 MeV/c, respectively. Thus, the production of antikaons in the one-step process (1) is expected to be enhanced when the nucleons emerge with a low relative momentum in the final state. The squared invariant energy s available in the first pN collision (1), the function $\lambda(x,y,z)$, and the squared invariant energy s_{NNK} of the final nucleons and kaon, appearing in (7)-(10), are defined as in ref. [1] by eqs. (18), (29), and (30), respectively. The in-medium antikaon momentum $\mathbf{p}'_{K^-}$ is related to the vacuum one $\mathbf{p}_{K^-}$ by eq. (24) from [1]. The "in-medium" total cross-section $\sigma_{pN\to NNKK^-}(\sqrt{s},\sqrt{s^*_{\rm th}})$ for the K^- production in reaction (1) appearing in (7) is equivalent to the vacuum cross-section $\sigma_{pN\to NNKK^-}(\sqrt{s},\sqrt{s_{\rm th}})$ [1], in which the free threshold $\sqrt{s_{\rm th}}$ is replaced by the effective threshold $\sqrt{s^*_{\rm th}}$. The latter is related to the vacuum threshold $\sqrt{s_{\rm th}} = 2(m_N + m_K)$ and to the mean-field potentials $U_{K^\pm}(\rho_N)$, $U_N(\rho_N)$ introduced above by eq. (20) from [1]. As in ref. [1], we will employ in our calculations of the antikaon production from the primary process (1) for the free total cross-section $\sigma_{pN\to NNKK^-}(\sqrt{s},\sqrt{s_{\rm th}})$ the fit (31) (from ref. [1]) of the available experimental data close to the threshold for the $pp \to ppK^+K^-$ reaction. Therefore, relevant pp-FSI effects in $\sigma_{pN\to NNKK^-}(\sqrt{s},\sqrt{s_{\rm th}})$ are automatically included. It should be noted that a special question regards the validity of the incorporation of the elementary NN-FSI effects into the analysis of $p+A$ reactions. The possible screening of these effects in the nuclear medium is an open subject, which has not yet been investigated theoretically. Since in the subthreshold energy region the outgoing nucleons are mainly emitted in the forward directions close to each other with small relative momenta and "laboratory" (relative to the target system) momenta, essentially greater than the Fermi momentum, one may hope that the bare NN-FSI is not drastically suppressed in nuclei, but only partially loses its strength here. The latter has been taken into account in our approach by using in (12) the effective nucleon mass m^*_N instead of the free one m_N. Since the total cross-section $\sigma_{pN\to NNKK^-}$ is proportional to the quantity I_4 in the near-threshold energy region, the energy dependence of the inclusive invariant cross-section (7) for a given kinematics (for fixed three-momentum of the produced antikaon) close to threshold $\sqrt{s_{NNK,\rm th}} = 2m^*_N + m^*_{K^+}$ is almost entirely governed by the medium-FSI-modified three-body phase-space integral (9). Equations (8), (9), (12) show that the relevant relative NN momentum q for fixed excess energy $\epsilon_{NNK} = \sqrt{s_{NNK}} - 2m^*_N - m^*_{K^+}$ varies from zero up to $q_{\rm max} \approx \sqrt{m^*_N\epsilon_{NNK}}$. For example, the momentum $q_{\rm max}$ is approximately equal to 100, 150, and 220 MeV/c at excess energies of 10, 25, and 50 MeV, respectively. Therefore, at beam energies far below the free threshold energy [3] of interest, where the corresponding excess energies ϵ_{NNK} are sufficiently small [4], the K^- production on nuclei from the primary reaction channel (1) will be enhanced (see below) due to the elementary pp-FSI compared to the calculation in [1] which does not include this FSI. In what follows we use eqs. (7)-(12) in our

[3] It is determined from the condition that $\sqrt{s_{NNK}} = 2m_N + m_K$ and, for instance, equals 2.99 GeV for the kinematics of the experiment in ref. [2] in which K^--mesons with a momentum of 1.28 GeV/c at a laboratory angle of 10.5° have been detected.

[4] Thus, for example, our estimates show that the main contribution to the K^- production in the primary process (1) at incident energy of 2.25 GeV for kinematics of the experiment in ref. [2] comes from the excess energies ϵ_{NNK} falling in the range between zero and approximately 50 MeV.

calculations of the antikaon production cross-sections on ^{9}Be, ^{63}Cu, and ^{197}Au target nuclei from the one-step reaction channel (1) in the framework of the model in [1]. For the K^- production calculations in the case of the ^{197}Au target nucleus reported here we used for the nuclear density $\rho_N(\mathbf{r})$ the Woods-Saxon distribution (35) from [1] with $R = 6.825$ fm and $a = 0.55$ fm [37]. The nucleon spectral function $P(\mathbf{p}_t, E)$ for this target nucleus is assumed to be the same as that for ^{208}Pb [38]. The latter was taken from [39].

Now let us briefly consider the two-step K^- production mechanism adopted in [1] . An incident proton can also produce a K^- through the following two-step production process:

$$p + N_1 \rightarrow N + N + \pi, \tag{13}$$

$$\pi + N_2 \rightarrow N + K + K^-. \tag{14}$$

Again, as in [1], we will use in the subsequent calculations of the K^- production cross-section from the secondary reaction channel (14) the same in-medium modifications of the masses of final hadrons (kaon, antikaon, and nucleon) as those (2) for hadrons from primary pN collisions due to the corresponding mean-field potentials $U_{K^\pm}(\rho_N)$ and $U_N(\rho_N)$. In the present work these potentials are assumed to be density-independent with depths $U^0_{K^\pm}$ and U^0_N taken at a nuclear saturation density. In line with the above-mentioned arguments, the FSI between the outgoing kaon and nucleon participating in the K^- production process (14) is assumed to be negligible due to the weakness of the KN interaction. As a result, we will calculate hereafter the K^- yield in pA collisions from the secondary channel (14) following strictly the approach [1]. It should be pointed out that in our calculations of the antikaon production from the pion-induced reaction channel (14) in the case of having ^{197}Au as target nucleus, which we present below, the ratio of the differential cross-section for the pion creation on this nucleus from the primary process (13) to the effective number of nucleons participating in it is supposed to be the same as that for ^{63}Cu adjusted to the kinematics of ^{197}Au.

Now, let us proceed to the discussion of the results of our calculations for antikaon production in p-Be, p-Cu, and p-Au interactions in the framework of the model outlined above.

3 Results

At first, we will concentrate on the reanalysis of the experimental data in ref. [2] on the K^- excitation functions for the $p + {}^{9}$Be and $p + {}^{63}$Cu reactions.

Figures 1 and 2 show a comparison of the calculated invariant differential cross-sections for the production of K^--mesons with a momentum of 1.28 GeV/c at a laboratory angle of 10.5° from the primary $pN \rightarrow NNKK^-$ and secondary $\pi N \rightarrow NKK^-$ channels with the data taken from the experiment in ref. [2], respectively, for $p + {}^{9}$Be and $p + {}^{63}$Cu reactions at various bombarding energies. It is seen again that, indeed, our old calculations in [1] for the primary antikaon production process (1) with the attractive nucleon and antikaon density-dependent mean-field potentials not including the FSI effects among the outgoing nucleons (thin solid lines in figs. 1, 2) substantially underestimate the far subthreshold data points [5]. Calculations in [1] for the secondary K^- production channel (14), when in-medium modifications of the masses of the outgoing antikaon and nucleon are included (thick solid lines in figs. 1, 2), essentially miss the data at all beam energies of interest. Additional inclusion of the FSI effects between the final nucleons participating in the primary production process (1) enhances the K^- yield from this process by about a factor of 2.5 and 1.2, respectively, at "low" ($\epsilon_0 = 2.2$ GeV) and "high" ($\epsilon_0 = 3.0$ GeV) incident

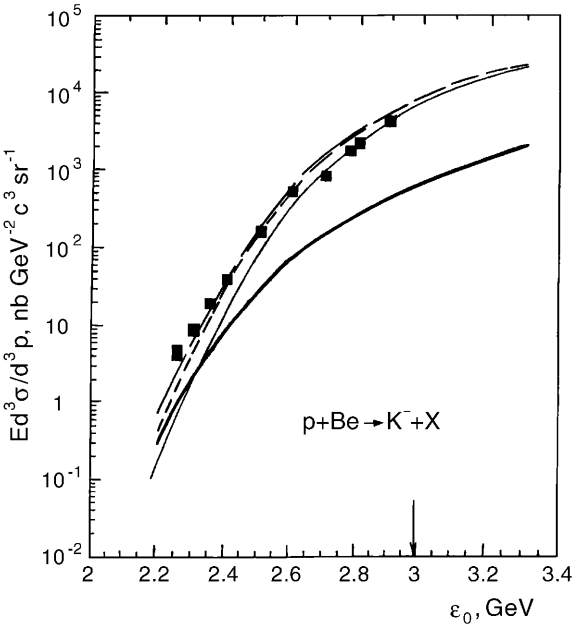

Fig. 1. Lorentz-invariant cross-sections for the production of K^--mesons with a momentum of 1.28 GeV/c at a lab angle of 10.5° in $p+{}^{9}$Be reactions as functions of the laboratory kinetic energy ϵ_0 of the proton. The experimental data (full squares) are from the experiment of ref. [2]. The curves show our calculation. The thin solid line shows the calculation in [1] for the primary production process (1) with the density-dependent potentials not including the FSI effects among the outgoing nucleons at $V_0 = 40$ MeV, $U_N(\rho_N) = -34(\rho_N/\rho_0)$ MeV, $U_{K^+}(\rho_N) = 0$, $U_{K^-}(\rho_N) = -126(\rho_N/\rho_0)$ MeV. The short-dashed line denotes the same calculation as the thin solid line, but this time including the FSI effects between the outgoing nucleons. The thick solid line shows the calculation in [1] for the secondary production process (14) at $U^0_N = -34$ MeV, $U^0_{K^+} = 0$, $U^0_{K^-} = -126$ MeV. The long-dashed line is the sum of the short-dashed and thick solid lines. The arrow indicates the threshold for the reaction $pN \rightarrow NNKK^-$ occuring on a free nucleon at the kinematics under consideration.

[5] It should be stressed that the additional application of the repulsive K^+ potential of about 20 MeV at a normal nuclear matter density ρ_0, as was shown in [1], does not allow us to describe the near-threshold data points either, and this counts in favor of the scenario with a zero kaon potential.

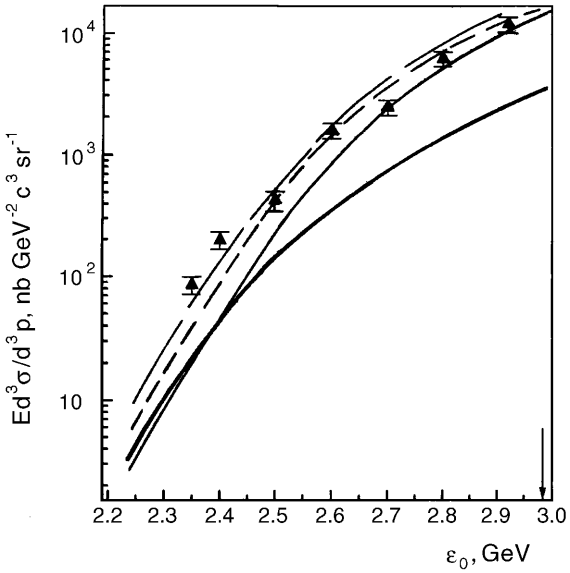

Fig. 2. Lorentz-invariant cross-sections for the production of K^--mesons with a momentum of 1.28 GeV/c at a lab angle of 10.5° in $p + {}^{63}$Cu reactions as functions of the laboratory kinetic energy of the proton. The experimental data (full triangles) are from the experiment in ref. [2]. The curves show our calculation. The notation of the curves and arrow are identical to those in fig. 1.

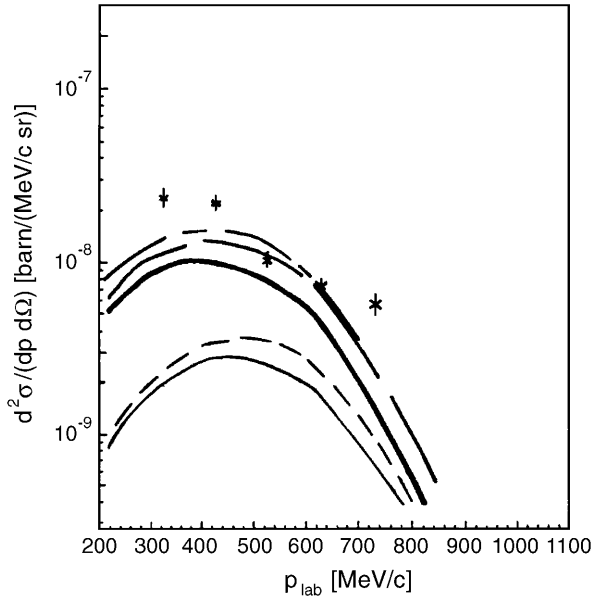

Fig. 3. Double differential cross-sections for the production of K^--mesons at a lab angle of 40° in the interaction of protons of energy 2.5 GeV with ^{197}Au nuclei as functions of antikaon momentum. The experimental data (crosses) are from the experiment in ref. [6]. The curves show our calculation. The thin solid line shows the calculation for the primary production process (1) with the density-dependent potentials not including the FSI effects among the outgoing nucleons at $V_0 = 40$ MeV, $U_N(\rho_N) = -34(\rho_N/\rho_0)$ MeV, $U_{K^+}(\rho_N) = 0$, $U_{K^-}(\rho_N) = -126(\rho_N/\rho_0)$ MeV. The short-dashed line represents the same as the thin solid line, but incorporating the FSI effects between the outgoing nucleons. The thick solid line shows the calculation for the secondary production process (14) at $U_N^0 = -34$ MeV, $U_{K^+}^0 = 0$, $U_{K^-}^0 = -126$ MeV. The long-dashed line is the sum of the short-dashed and thick solid lines. The line with alternating short and long dashes shows the same as the long-dashed line, but the deep K^- optical potential of depth 200 MeV, extracted [40–42] from the kaonic atom data, is used instead of a relatively deep potential of depth 126 MeV.

energies (compare short-dashed and thin solid lines in figs. 1, 2), as well as brings the theoretical predictions in much better agreement (especially at energies ≤ 2.6 GeV) with the experimental data [6]. Moreover, adding to the antikaon yield in the latter case also the contribution from the pion-induced channel (14) results in a very good description (long-dashed lines) of the data [2]. The good agreement with these data achieved in our present calculations indicates that the use of the elementary NN-FSI effects in $p + A$ reactions seems quite reasonable. On the other hand, it leaves a minor room for the K^- production via higher-order processes such as, for example, collisions of the initial proton with nucleon clusters. Figures 1 and 2 also illustrate that the two-step (thick solid line) to one-step (short-dashed line) K^- production cross-section ratio increases with decreasing incident energy down to 2.2 GeV. In the present model calculations this ratio is about 1/1.8 and 1/1.6 at "low" kinetic energies ($\epsilon_0 \approx 2.2$–2.3 GeV), about 1/4.5 and 1/2.5 at "intermediate" incident energies ($\epsilon_0 \approx 2.4$–2.5 GeV), about 1/12 and 1/5 at "high" beam energies ($\epsilon_0 \approx 2.7$–2.9 GeV), respectively, for ^{9}Be and ^{63}Cu target nuclei. This demonstrates that the proton-induced reaction channel clearly dominates the K^- production only at bombarding energies ≥ 2.4 GeV, whereas at lower incident energies its dominance, contrary to the results in [1], is less pronounced.

Now let us focus on the analysis of the experimental data [6] on the K^- spectrum from $p + {}^{197}$Au interactions.

Figure 3 shows the results of our calculations for the double differential cross-sections for the production of K^--mesons from the primary $pN \to NNKK^-$ and secondary $\pi N \to NKK^-$ channels at an angle of 40° in the interaction of protons of energy 2.5 GeV with ^{197}Au nuclei and together with the preliminary experimental data of ref. [6]. If we adopt the same in-medium nucleon and antikaon optical potentials and use the elementary NN-FSI effects, which allowed us to describe the above data on the antikaon excitation functions [2], our full calculations (the sum of the results obtained both for primary and secondary antikaon production processes, long-dashed line in fig. 3) reproduce reasonably well the data of ref. [6]. Using in the calculation a deep K^- optical potential of depth 200 MeV, extracted from the kaonic atom data, instead of a relatively deep potential of depth 126 MeV (the line with alternating short and long dashes) leads to a better description of the experimental data at antikaon momenta ≤ 0.5 GeV/c. This counts in favor of the conclusion that

[6] It should be emphasized that the inclusion only of the NN-FSI effects alone in calculating the K^- yield from the primary process (1) does not allow one to describe these data.

the K^- nuclear potential can be as attractive as that derived from the kaonic atom studies [40–42]. To make more reliable conclusions on the actual magnitude of the K^- optical potential in nuclear matter, we strongly need further measurements of differential cross-sections for the K^- production in pA collisions at low antikaon momenta. Inconsistently with our previous findings of figs. 1, 2, the inclusion of only the $pN \to NNKK^-$ channel substantially underpredicts the data (see fig. 3), and the majority of antikaons stem, in the heavy target nucleus, from the pion-induced process $\pi N \to NKK^-$. The latter channel is dominant in the kinematics under consideration. So, it becomes evident that, while the FSI among the final nucleons participating in the one-step process (1) increases (by a factor of about 1.4) the K^- production cross-section from this process (compare short-dashed and thin solid lines), it nevertheless only slightly contributes to the total antikaon yield. This is contrary to the preceding cases where the process (1) is found to be of importance.

Finally, in fig. 4 we show the predictions of the above model for the Lorentz-invariant inclusive cross-sections for the production of K^--mesons at a laboratory angle of 10.5° from the proton- and pion-induced reaction channels for $p + {}^9\mathrm{Be} \to K^- + X$ reaction at 2.25 GeV beam energy. The data point [7] at 1.28 GeV/c was taken from [2]. It can be seen that the inclusion of the FSI effects among the outgoing nucleons participating in the one-step process (1) (short-dashed line in the top panel) enhances the high-momentum part ($p_{\mathrm{lab}} \geq 0.8$ GeV/c) of the antikaon spectrum from this process by a factor of about 1.2–2.5 and practically does not affect its low-momentum part ($p_{\mathrm{lab}} \leq 0.6$ GeV/c). As a result, our overall calculations (the sum of contributions both from the one-step (1) and from the two-step (13), (14) reaction channels, long-dashed line in the bottom panel of fig. 4) reproduce quite well the measured K^- double differential cross-section at 1.28 GeV/c (cf. fig. 1) [2]. It is also clearly seen that the low-momentum parts of the antikaon spectra from the one-step and two-step production mechanisms react sensitively to the K^- potential at antikaon momenta $p_{\mathrm{lab}} \approx 0.2$–$0.3$ GeV/c. The K^- yields here are about a factor of 2–3 larger when a deep potential of depth 200 MeV [40–42] is applied compared to a shallow one with a central depth of 55 MeV, predicted very recently by the self-consistent chirally motivated coupled-channel approach [43] (compare three-dot and dotted lines in the top and bottom panels of fig. 4). This gives an opportunity, as was also noted before [1,44,45], to determine the K^- potential in nuclear matter experimentally (to distinguish at least between shallow and deep K^- optical potentials) by measuring differential cross-sections for subthreshold "soft" (low-momentum) antikaon production on different target nuclei. Figure 4 shows that the two-step (thick solid line) to one-step (short-dashed line) K^- creation cross-section ratio is about 2.5/1 and 1/3, respectively, at low ($p_{\mathrm{lab}} \approx 0.2$–$0.4$ GeV/c) and high ($p_{\mathrm{lab}} \approx 0.8$–$1.0$ GeV/c) antikaon momenta. This indicates the dominance of the one-step and two-step K^- production mechanisms,

[7] It corresponds to the lowest data point in fig. 1.

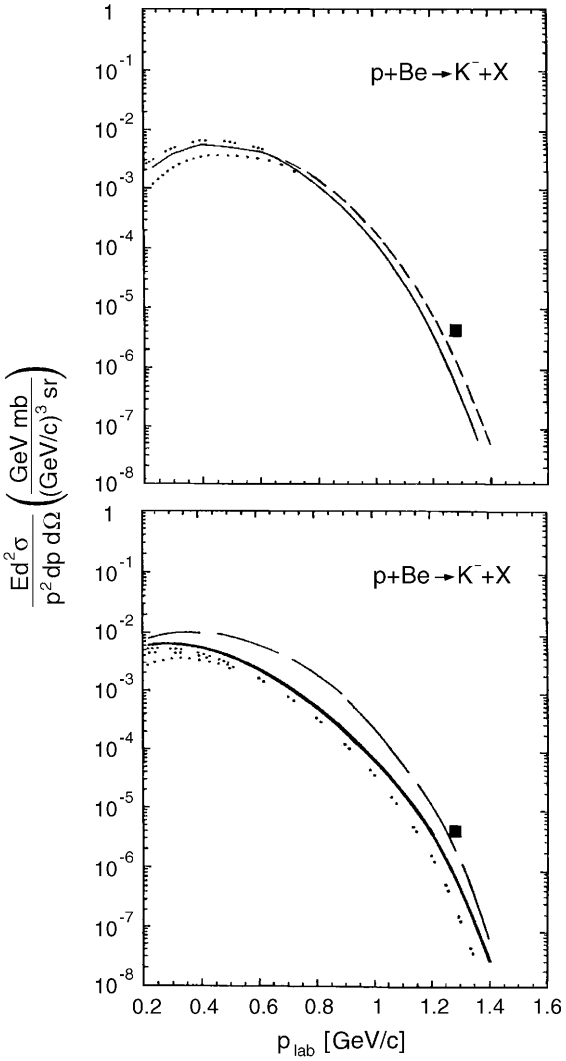

Fig. 4. Lorentz-invariant inclusive cross-sections for the production of K^--mesons at a laboratory angle of 10.5° in the interaction of 2.25 GeV protons with the ^{9}Be nuclei as functions of antikaon momentum. The experimental data point at 1.28 GeV/c (full square) is from the experiment in ref. [2]. The curves show our calculation for the primary and secondary K^- production processes. Top: the thin solid line is the calculation for the primary production process (1) with the density-dependent potentials not including the FSI effects among the outgoing nucleons at $V_0 = 40$ MeV, $U_N(\rho_N) = -34(\rho_N/\rho_0)$ MeV, $U_{K^+}(\rho_N) = 0$, $U_{K^-}(\rho_N) = -126(\rho_N/\rho_0)$ MeV. The dotted and three-dot lines denote the same as the thin solid line, but using, respectively, the shallow antikaon potential $U_{K^-}(\rho_N) = -55(\rho_N/\rho_0)$ MeV and the deep one, extracted [40–42] from the kaonic atom data, instead of a relatively deep potential of depth 126 MeV. The short-dashed line denotes the same as the thin solid line, but incorporates the FSI effects between the outgoing nucleons. Bottom: the dotted, two-dot, three-dot, and thick solid lines are calculations for the secondary production process (14) at $U_N^0 = 0$, $U_{K^+}^0 = 0$, $U_{K^-}^0 = -55$ MeV; $U_N^0 = 0$, $U_{K^+}^0 = 0$, $U_{K^-}^0 = -126$ MeV; $U_N^0 = 0$, $U_{K^+}^0 = 0$, $U_{K^-}^0 = -200$ MeV; and $U_N^0 = -34$ MeV, $U_{K^+}^0 = 0$, $U_{K^-}^0 = -126$ MeV, respectively. The long-dashed line is the sum of the short-dashed (depicted in the top panel) and thick solid lines.

correspondingly, in the "hard" and "soft" subthreshold antikaon production in p-^{9}Be collisions. It should be, however, stressed that the latter is in line with the findings inferred above (see figs. 1-3) about the role played by the direct K^- production mechanism in the subthreshold "hard" and "soft" antikaon creation, respectively, in p-^{9}Be, p-^{63}Cu interactions [2] and in p-^{197}Au collisions [6].

Taking into account the above considerations, we may conclude that the FSI effects between the nucleons originating from the primary K^- production channel (1) are quite important in order to describe the experimental data [2] on the "hard" antikaon creation in p-^{9}Be and p-^{63}Cu interactions within the approach [1] when the influence of the nuclear density-dependent nucleon and antikaon mean-field potentials on this channel is included. On the other hand, these effects are found to be negligible in reproducing the data [6] on the K^- production in p-^{197}Au collisions due to the dominance here, contrary to the measurements [2], of the secondary pion-induced reaction channel (14).

4 Conclusions

In this paper we reanalyze the experimental data [2] on antikaon excitation functions for $p + {}^9$Be and $p + {}^{63}$Cu reactions and analyze the data [6] on the K^- spectrum from $p + {}^{197}$Au interactions in the subthreshold energy regime using a spectral function approach [1]. It has been modified to account for the final-state interaction between the outgoing nucleons participating in the primary proton-nucleon production process. The nucleon-nucleon final-state–interaction correction of the invariant inclusive cross-section for the antikaon production in this process was made in line exactly with the Watson-Migdal theory of the FSI adopting the inverse Jost-function method. It was shown that this correction is important for reproducing the energy dependences [2] of the Lorentz-invariant cross-sections for the "hard" K^- production in p-^{9}Be and p-^{63}Cu collisions within the present approach when the influence of the nuclear density-dependent nucleon and antikaon effective potentials on the proton-induced reaction channel is included. On the other hand, it was found to play a negligible role in describing the data [6] on the spectrum of relatively soft antikaons from p-^{197}Au interactions at an incident energy of 2.5 GeV. In this case, contrary to those mentioned above, the pion-induced reaction channel turned out to be dominant and, therefore, only the attractive nucleon and antikaon mean fields were essential. The good agreement with the experimental data obtained within the present approach favors the possibility to employ the elementary NN-FSI effects in $p + A$ reactions, as well as leaves a minor room for the subthreshold K^- production via other mechanisms in these reactions.

Consistent with the previous findings in [1], our present results show also strong sensitivity of the "soft" K^- production in pA interactions at subthreshold incident energies to the in-medium antikaon optical potential. According to them, the measurements of differential cross-sections for the K^- creation on different target nuclei are most promising at antikaon momenta $p_{\rm lab} \leq 400$ MeV/c to distinguish between shallow and deep antikaon potentials. The experimental data [6] available presently in the indicated momentum range favor a deep K^- optical potential. However, these data are poor to draw more definite conclusions on the actual magnitude of the K^- potential in nuclear medium. Therefore, further measurements of the low-momentum antikaon production in pA collisions at subthreshold beam energies are needed nowadays to get a better understanding of the K^- properties in nuclear matter.

The author is grateful to Yu.T. Kiselev and V.A. Sheinkman for their interest in the work.

References

1. E.Ya. Paryev, Eur. Phys. J. A **9**, 521 (2000).
2. A.V. Akindinov, M.M. Chumakov, Yu.T. Kiselev *et al.*, Preprint ITEP 41-99 (Moscow, 1999).
3. K.M. Watson, Phys. Rev. **88**, 1163 (1952).
4. M.L. Goldberger, K.M. Watson, *Collision Theory* (Wiley, New York, 1964).
5. A.B. Migdal, JETP **1**, 2 (1955).
6. W. Scheinast (for the KaoS Collaboration), Acta Phys. Pol. B **31**, 2305 (2000).
7. C. Hanhart, K. Nakayama, Phys. Lett. B **454**, 176 (1999).
8. J.A. Niskanen, Phys. Lett. B **456**, 107 (1999).
9. V.V. Baru, A.M. Gasparian, J. Haidenbauer *et al.*, nucl-th/0006075; Yad. Fiz. **64**, 633 (2001).
10. F. Kleefeld, Acta Phys. Pol. B **31**, 2225 (2000).
11. B.J. Morton, E.E. Gross, E.V. Hungerford *et al.*, Phys. Rev. **169**, 825 (1968).
12. H.P. Noyes, H.M. Lipinski, Phys. Rev. C **4**, 995 (1971).
13. J.P. Naisse, Nucl. Phys. A **278**, 506 (1977).
14. A. Moalem, L. Razdolskaja, E. Gedalin, hep-ph/9505264.
15. G. Fäldt, C. Wilkin, Phys. Lett. B **382**, 209 (1996).
16. G. Fäldt, C. Wilkin, Phys. Rev. C **56**, 2067 (1997).
17. G. Fäldt, C. Wilkin, Z. Phys. A **357**, 241 (1997).
18. C. Wilkin, *Final-State Interaction Theory*, Presentation at the ANKE Collaboration Meeting, 20 February 2001, unpublished.
19. A. Sibirtsev, W. Cassing, nucl-th/9802025.
20. J.T. Balewski, A. Budzanowski, H. Dombrowski *et al.*, Phys. Lett. B **388**, 859 (1996).
21. J.T. Balewski, A. Budzanowski, C. Goodman *et al.*, Eur. Phys. J. A **2**, 99 (1998).
22. V. Bernard, N. Kaiser, Ulf-G. Meissner, Eur. Phys. J. A **4**, 259 (1999).
23. N. Kaiser, nucl-th/9907114.
24. N. Kaiser, Eur. Phys. J. A **5**, 105 (1999).
25. P. Moskal, H.H. Adam, J.T. Balewski *et al.*, Phys. Lett. B **482**, 356 (2000).
26. A.V. Akindinov, M.M. Chumakov, Yu.T. Kiselev *et al.*, Preprint ITEP 37-99 (Moscow, 1999).
27. B.L. Druzhinin, A.E. Kudryavtsev, V.E. Tarasov, Z. Phys. A **359**, 205 (1997).
28. R. Shyam, U. Mosel, Phys. Lett. B **426**, 1 (1998).
29. A. Sibirtsev, W. Cassing, Eur. Phys. J. A **2**, 333 (1998).
30. A. Sibirtsev, W. Cassing, nucl-th/9904046.

31. R. Shyam, Phys. Rev. C **60**, 055213 (1999).
32. A. Sibirtsev, K. Tsushima, W. Cassing, A.W. Thomas, nucl-th/0004022.
33. A.I. Titov, B.Kämpfer, B.L. Reznik, Eur. Phys. J. A **7**, 543 (2000).
34. P. Moskal, H.H. Adam, A. Budzanowski *et al.*, nucl-ex/0007018.
35. V. Abaev, V. Koptev, H. Ströher, Preprint PNPI 2403 (Gatchina, 2001).
36. O. Dumbrajs, R. Koch, H. Pilkuhn *et al.*, Nucl. Phys. B **216**, 277 (1983).
37. A. Sibirtsev, W. Cassing, nucl-th/9909053.
38. C. Ciofi degli Atti, S. Simula, Phys. Rev. C **53**, 1689 (1996).
39. E.Ya. Paryev, Eur. Phys. J. A **7**, 127 (2000).
40. E. Friedman, A. Gal, C.J. Batty, Phys. Lett. B **308**, 6 (1993).
41. E. Friedman, A. Gal, C.J. Batty, Nucl. Phys. A **579**, 518 (1994).
42. E. Friedman, Nucl. Phys. A **639**, 511c (1998).
43. A. Cieply, E. Friedman, A. Gal, J. Mares, nucl-th/0104087.
44. A. Sibirtsev, W. Cassing, Nucl. Phys. A **641**, 476 (1998).
45. Yu.T. Kiselev (for the FHS Collaboration), J. Phys. G **25**, 381 (1999).